European Conference on Optical Communication (ECOC) 2022 © Optica Publishing Group 2022

Full-Duplex Bidirectional Indoor Steerable OWC System using Orthogonal Polarization States

N.Q. Pham(1), K.A. Mekonnen(1), A. Mefleh(2), A.M.J. Koonen(1), E. Tangdiongga(1)

(1) Electro-Optical Communication Systems, Faculty of Electrical Engineering, Eindhoven University of Technology, The Netherlands, n.q.pham@tue.nl
(2) KPN, Technology Innovation, Roadmap & Architecture, Maanplein 55, The Hague, The Netherlands

Abstract *To avoid beam-steering at users, we propose the use of same wavelength for down and upstream to realize a full-duplex bidirectional architecture using off-the-shelf XFP transceivers. Symmetric data rate of 10 Gbps is experimentally demonstrated by implementing orthogonal polarization states to mitigate the reflection crosstalk. ©2022 The Author(s)*

Introduction

The ever-increasing growth in the demand for wireless traffic is triggering the shortage of radio spectrum. In recent years, researchers have been focusing on optical wireless communication (OWC) as a promising candidate for the future 6G networks and beyond [1]. Recently, much attention has been paid to improving the downstream regarding steering technique, capacity, and receiver's field-of-view (FoV). Beams can be steered wavelength-transparently using active elements such as MEMS mirrors [2] or spatial light modulators [3], or wavelength-dependently using passive elements such as a pair of crossed gratings [4] or an arrayed waveguide grating router (AWGR) [5]. Wide FoV optical wireless receivers were proposed using a matrix of photodiodes [6] or a re-configurable intelligent surface [7].

As a next step, main network functionalities such as bi-directionality and reconfigurability need to be addressed because such functions are the keys to realizing cost efficiency, full-duplex transmission, and mobility. Often, the upstream requires a separate channel on the user device (UD) side, such as a wireless radio technique [8] or near-infrared wide beam [9]. Consequently, the upstream has a lower channel capacity and a broad beam profile, which raises the trade-off between the link budget and bandwidth or needs upstream steering.

This study proposes a new full-duplex bidirectional OWC system. The downstream is based on the AWGR-based beam steering, which was demonstrated successfully in our previous study [5]. We focus on establishing the upstream by utilizing the principle of reversibility of the downstream without an additional steering device. We exploit an orthogonal polarization-based technique to realize high-speed multi-Gbps bidirectional transmission. Moreover, an automatic tuning scheme is proposed to lock the upstream wavelength to the downstream wavelength, so the optical upstream signal can propagate reversely through the AWGR.

Bidirectional OWC System

Our OWC system concept is depicted in Fig. 1. The optical antenna consisting of an AWGR-based beam steering module controls the emitting direction of downstream beams based on their wavelength. A detailed study of the beam-steering mechanism was presented in [5]. Besides, to determine the exact position of UDs that needs to be projected, a camera-based localization was proposed in our previous work [10]. On the UD side, the receiver is made of a collimator, a tunable XFP, and an automatic alignment actuator [11].

Here, we propose an upstream OWC architecture to realize a bidirectional high-capacity transmission. The upstream optical link is based on two principles. The first is based on the principle of reversibility of optical paths. The upstream link propagates in the same path as the downstream with the reversed direction. Thus, the UD needs no additional beam-steering device, but the UD should be kept aligned to the optical antenna. We deploy two circulators at the optical antenna and the UD to separate the downstream and the upstream based on the transmission direction. Secondly, we develop an automatic searching algorithm to tune the correct wavelength for XFP transceiver at the user side.

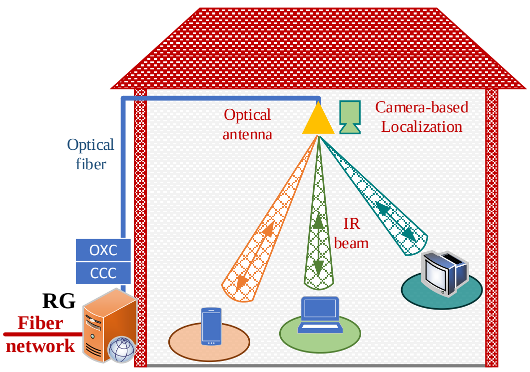

Fig. 1: Indoor steerable narrow beam OWC system.

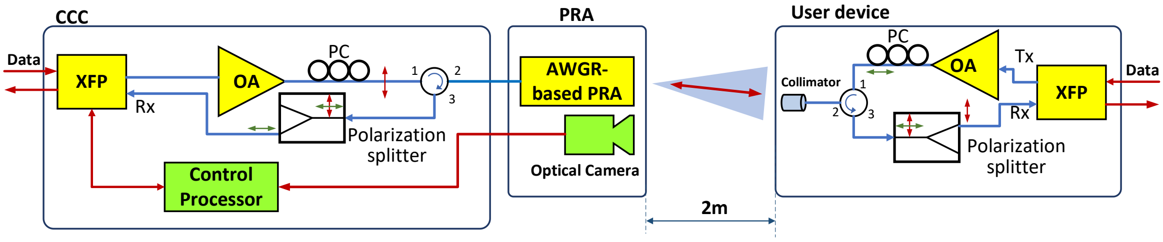

Fig. 2: Bidirectional full-duplex OWC architecture.

However, the proposed upstream architecture raises challenges of power loss and reflection crosstalk. To achieve a good fill factor of the covered area with a limited number of wavelengths, a defocusing approach was applied to widen the beam's footprint. A collimator was used to focus the optical beam to the single-mode fiber (SMF) on the UD side. Because the beam diameter is much larger than the lens' diameter, the transmission loss mainly depends on the coupling factor between the communication beam and the SMF. Theoretically, when applying an aberration-free thin lens for a beam with uniformly distributed intensity, the coupling factor T of the beam power P onto the SMF is

$$T = \begin{cases} \cos\alpha\left(\frac{D_1}{D_0}\right)^2 & \alpha \le \alpha_{max} \\ 0 & \alpha > \alpha_{max} \end{cases} \quad (1)$$

where α is the incident angle of the beam, α_{max} is the FoV angle, D_0 is the beam diameter, and D_1 is the lens diameter. Furthermore, the transmitted power is limited for eye-safety, the loss will cause the received power to be below the receiver sensitivity for multi-Gbps capacity.

In addition, in fiber-to-free-space applications, Fresnel reflections typically occur at the glass-to-air interface at the fibre-end because of the refraction index mismatch. These reflections are much worse than comparable values for fiber-to-fiber coupling. The reflectivity can be calculated using the following formula, assuming normal incidence

$$R = \left(\frac{n_0 - n_s}{n_0 + n_s}\right)^2 \quad (2)$$

where R is the reflectivity, n_0 is the refractive index of air, and n_s is the refractive index of the fiber core. Thus, part of the optical signal is reflected back to the light source instead of exiting the fiber, causing interference to the co-propagating upstream or downstream signals.

Operational Principle

We propose a polarization division method to mitigate the impact of crosstalk from the reflected signal on the copropagating desired signals. Fig. 2 shows the operating principle, in which the down and the upstream signal are polarized into two orthogonal states by polarization controllers. Let's elaborate on the upstream performance with $E_{c,x}^u$ and $E_{s,x}^u$ as the carrier and signal of the upstream with x-polarization state, $E_{c,y}^d$ and $E_{s,y}^d$ as the carrier and signal of the upstream with y-polarization and $E_{c,y}^{dr}$ and $E_{s,y}^{dr}$ as the reflected carrier and reflected signal of the downstream. The XFP detects the upstream signal at the UD, and the photocurrent can be presented as

$$I = \left|E_{c,x}^u + E_{s,x}^u + E_{c,y}^{dr} + E_{c,y}^{dr}\right|^2 \quad (3)$$

Because two orthogonal polarization states do not affect each other upon detection, we have

$$\begin{aligned} I &= \left|E_{c,x}^u + E_{s,x}^u\right|^2 + \left|E_{c,y}^{dr} + E_{c,y}^{dr}\right|^2 \\ &= \left|E_{c,x}^u\right|^2 + \left|E_{s,x}^u\right|^2 + 2Re\left(E_{c,x}^u E_{s,x}^{u\,*}\right) \\ &+ \left|E_{c,y}^{dr}\right|^2 + \left|E_{c,y}^{dr}\right|^2 + 2Re\left|E_{c,y}^{dr} E_{c,y}^{dr\,*}\right| \end{aligned} \quad (4)$$

The first item $\left|E_{c,x}^u\right|^2$ is the DC generated by the target carrier, which does not affect the signal. The second item $\left|E_{s,x}^u\right|^2$ is the inherent signal-to-signal beat interference (SSBI) generated by the target signal, and the third item $2Re\left(E_{c,x}^u E_{s,x}^{u\,*}\right)$ is the recovered signal. The SSBI item is a noise that reduces the signal-to-noise ratio of the system. In a typical IM-DD system, the optical carrier is high-power-biased to suppress its inherent SSBI; thus, $E_{c,x}^u \gg E_{s,x}^u$. The other items are crosstalk. Due to the filtering of the polarization beam splitter (PBS), the cross signal is much smaller than the target signal $E_{s,y}^{dr} \ll E_{s,x}^u$ at the x-polarization output of the PBS. Thus, all electrical crosstalk items can be neglected. For the downstream channel, similar results can be obtained.

Furthermore, we implemented an automatic algorithm to tune the correct wavelength for the upstream, as depicted in Fig. 3. After localizing the UD, the central communication controller (CCC) sends a request to the UD to start a wavelength scanning. Each wavelength is transmitted in one slot of time. Due to the filtering of the AWGR, only the correct wavelength can be propagated inversely through the AWGR and received by the XFP at the CCC. Then the CCC

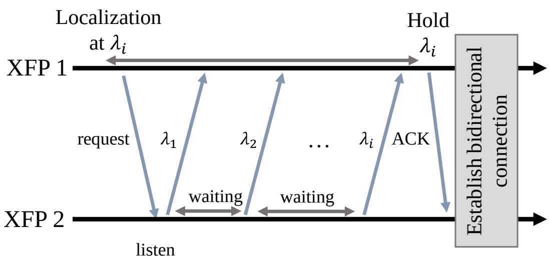

Fig. 3: Automatic wavelength-locking flow.

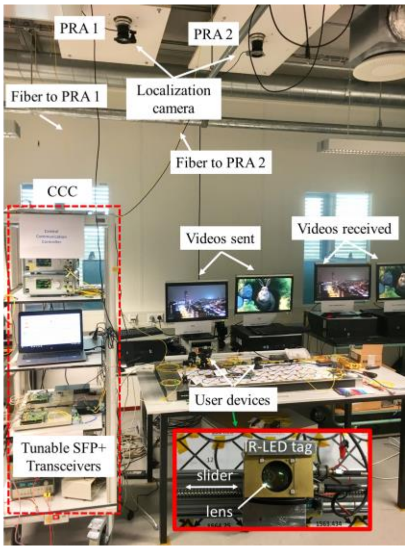

Fig. 4: Experimental setup.

sends an ACK signal to the UD to stop the scanning and lock the wavelength. Thus, the bidirectional OWC transmission is initiated.

Experiments and Results

Fig. 4 shows the experimental setup to evaluate our proposed bidirectional OWC system. At a reach of 2.5 m, each optical antenna covered a wide area of 1.6 m × 1.6 m. Two tunable XFP transceivers with an ITU grid channel spacing of 50 GHz were deployed. Finisar evaluation boards were used to module an on-off-keying non-return-to-zero 10 Gbps signal with pseudorandom binary sequence of 2^{23}-1 through the high-speed electrical interface SFI. Note that at the time of validation, only 10 Gbps platform was available but the concept can also work for higher data rates as there is no electrical bandwidth limitation in the link. The XFP transceivers were tuned by using the 2-wire interface. In addition, we used the low-speed contacts for control and status of the XFP, as Tx_Disable and Rx loss of signal (Rx_LOS), to send requests and monitor responses. The control plane managed the time slotting assignments for down and upstream communications.

Fig. 5a shows the transmission loss of the system and the reflection loss within the C-band wavelength with the mean of 29 dB and 30.2 dB, respectively. The high power loss was due to the footprint of the beam being much larger than the area of the lens and SMF. We need a large footprint to a good fill factor of the covered area, so the high power loss is unavoidable. Then, we evaluated the upstream performance in the presence of the reflection crosstalk from the downstream. The transmitted powers of the downstream and upstream were limited to 10 dBm for eye-safety. Without the polarization division, the ratio between the signal and the reflection was measured at most 1.5 dB because the maximum output for the upstream is also at 10 dBm. Thus, no signal was received. By implementing the polarization division scheme, the signal to crosstalk ratio was enhanced significantly. SMF, in place of the free space for the same configurations, was also performed as back-to-back measurements. Fig. 5b shows the measured results of the bit error rate at 5 and 10 Gbps. Although the proposed scheme introduced a penalty of 1 and 1.5 dB for BER <10^{-12} at 5 and 10 Gbps transmissions, respectively, the error-free transmissions were achieved with the upstream transmitted power at 1 and 3.5 dBm for the 5 and 10 Gbps.

Fig. 5c shows the captured signals of the automated tuning process. A user device was placed at the cell corresponding to the wavelength at ITU channel 10. We set the time slot for each wavelength to be 20ms. From the Rx_LOS signal of the XFP transceivers, the bidirectional OWC transmission has successfully established after 500 ms.

Conclusion

We presented a dynamic all-optical bidirectional indoor OWC system employing off-the-shelf XFP transceivers and an orthogonal polarization scheme to provide a simple, flexible, and easy solution. Symmetric transmission at data rates of at least 10 Gbps was feasible with an auto-pairing time of fewer than 2 seconds.

This work has been carried out in the framework of the TU/e-KPN flagship Smart-One program.

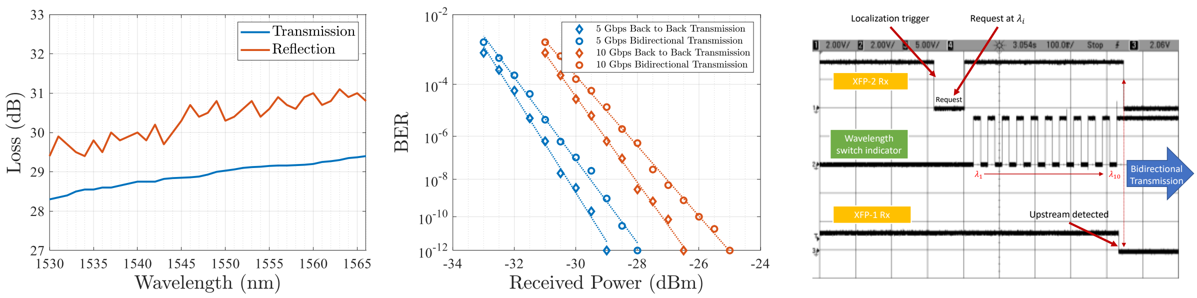

a) b) c)

Fig. 5: a) Transmission and reflection loss; b) BER performance at 5 Gbps and 10 Gbps transmissions for back-to-back and crosstalk with the polarization division scheme; c) Captured signals of auto tuning processing.

References

[1] K. Wang, T. Song, Y. Wang, C. Fang, A. Nirmalathas, C. Lim, E. Wong, and S. Kandeepan, "Evolution of Short-Range Optical Wireless Communications," in *2022 Optical Fiber Communications Conference and Exhibition (OFC)*, 2022, pp. 1–24.

[2] Y. Hong, F. Feng, K. R. Bottrill, N. Taengnoi, R. Singh, G. Faulkner, D. C. O'Brien, and P. Petropoulos, "Beyond terabit/s wdm optical wireless transmission using wavelength-transparent beam tracking and steering," in *Optical Fiber Communication Conference*, 2020, pp. W1G-4.

[3] Y. Feng, Y. Zhao, L. Yang, X. Wang, G. Zhuang, and R. Guo, "High-precision channel spacing and balanced output multiwavelength laser array with fine tunability," *Appl. Opt.*, vol. 60, no. 2, pp. 470–475, 2021.

[4] T. Koonen, J. Oh, K. Mekonnen, Z. Cao, and E. Tangdiongga, "Ultra-high capacity indoor optical wireless communication using 2D-steered pencil beams," *J. Light. Technol.*, vol. 34, no. 20, pp. 4802–4809, 2016.

[5] T. Koonen, K. Mekonnen, Z. Cao, F. Huijskens, N. Q. Pham, and E. Tangdiongga, "Ultra-high-capacity wireless communication by means of steered narrow optical beams," *Philos. Trans. R. Soc. Math. Phys. Eng. Sci.*, vol. 378, no. 2169, p. 20190192, Apr. 2020, doi: 10.1098/rsta.2019.0192.

[6] T. Koonen, K. A. Mekonnen, Z. Cao, F. Huijskens, N. Q. Pham, and E. Tangdiongga, "Beam-Steered optical wireless communication for industry 4.0," *IEEE J. Sel. Top. Quantum Electron.*, vol. 27, no. 6, pp. 1–10, 2021.

[7] A. R. Ndjiongue, T. M. Ngatched, O. A. Dobre, and H. Haas, "Toward the use of re-configurable intelligent surfaces in VLC systems: Beam steering," *IEEE Wirel. Commun.*, vol. 28, no. 3, pp. 156–162, 2021.

[8] K. A. Mekonnen, Z. Cao, N. Calabretta, E. Tangdiongga, and A. M. J. Koonen, "50 Gb/s indoor optical wireless communication equipped with millimeter-wave backup system and localization and tracking," in *2017 European Conference on Optical Communication (ECOC)*, 2017, pp. 1–3.

[9] C. Chen, D. A. Basnayaka, A. A. Purwita, X. Wu, and H. Haas, "Wireless infrared-based LiFi uplink transmission with link blockage and random device orientation," *IEEE Trans. Commun.*, vol. 69, no. 2, pp. 1175–1188, 2020.

[10] N. Pham, K. A. Mekonnen, E. Tangdiongga, A. Mefleh, and A. Koonen, "Multi-user localization and upstream signaling for indoor OWC system using a camera technology," in *Optical Fiber Communication Conference*, 2020, pp. M1J-7.

[11] N. Q. Pham, K. Mekonnen, E. Tangdiongga, A. Mefleh, and T. Koonen, "Auto-Aligned OWC Receiver for Indoor Mobile Users using Gradient Descent Algorithm," *OFC 2021*, vol. Tu5E.5, 2021.